View metadata, citation and similar papers at core.ac.uk

brought to you by CORE

provided by CiteSeerX

Australian Journal of Basic and Applied Sciences, 8(17) November 2014, Pages: 187-195

AENSI Journals

Australian Journal of Basic and Applied Sciences

ISSN:1991-8178

Journal home page: www.ajbasweb.com

Role of Magnetic Resonance Spectroscopy in Follow up Brain Tumors after Treatment

[1]H. Kamal, [1]M.T.Y. Tadros, [2]Sabry El-Mogy, [1]Salwa Nasr

[1]*Physics Dept., Faculty of Science, Mansoura Univ., Mansoura, 35516, Egypt.*
[2]*Radiology Dept., Faculty of Medicine, Mansoura Univ., Mansoura, 35516, Egypt*

ARTICLE INFO

Article history:
Received 19 August 2014
Received in revised form
19 September 2014
Accepted 29 September 2014
Available online 8 November 2014

Keywords:
MRS, metabolites, tumors, voxel, treatment.

ABSTRACT

Background: [1]H magnetic resonance spectroscopy (MRS) is an analytical method that enables the identification and quantification of metabolites in samples. It differs from conventional Magnetic Resonance Imaging (MRI) in that spectra provide physiological and chemical information instead of anatomy. MRS imaging allows a valuable insights into brain tumors characteristics, grads, and progression then follow up during treatments. Typically in MRS a single spectrum is acquired by averaging enough spectra over a long acquisition time. Averaging is necessary because of the complex spectral structures and relatively low concentrations of many brain metabolites, which result in a low signal-to-noise ratio (SNR) in MRS of a living brain. **Objective:** In this paper, acquiring and analyzing multivoxel MRS data are reviewed by calculating the areas under different peaks then compared with that obtained directly from 1H-MRS machine. 1H-MRS measurements of amounts of Choline (Cho), creatine (Cr) and N-acetylaspartate (NAA) relative to Cho, NAA and Cr in healthy brain tissue of a normal control brain tissue, and in the tissue of tumor of patient who had taken radiation therapy sessions. **Results:** The obtained results show a good agreement between the data obtained directly from MRS machine and that calculated from their spectra. This method is now used for to insure that these obtained spectra are calibrated with that obtained directly from MRS machine. So these may reflect the small changes in metabolites during treatment and follow up. Conclusion: The MRS data are seen to provide unique information that when combined with high-quality anatomical MR images has implications for defining tumor type and grade, directing biopsy or surgical resection, planning focal radiation or biological therapies, and understanding the mechanisms of success and failure of new treatments.

© 2014 AENSI Publisher All rights reserved.

To Cite This Article: H. Kamal, M.T.Y. Tadros, Sabry El-Mogy, Salwa Nasr, Role of Magnetic Resonance Spectroscopy in Follow up Brain Tumors after Treatment, ***Aust. J. Basic & Appl. Sci.,*** *8(17): 187-195, 2014*

INTRODUCTION

Magnetic resonance spectroscopy (MRS) technique, like magnetic resonance imaging (MRI), is based on the principle of nuclear magnetic resonance (NMR) (Gujar, Maheshwari *et al*. 2005). This technique can be theoretically being performed to most of the human body tissues but the human brain is the most important organ of interest for these studies. This may because that the human brain has a homogenous tissue structure and problems related to motion artifacts are very limited, thus make MRS technique is easily acceptable. MRS provides a non-invasive diagnostic tool (Chiang, Hsieh *et al*. 2014) for the biochemical characterization of path physiological processes in the brain.

Over the years, scientists have obtained MR spectra using a variety of nuclei including phosphorus (^{31}P), carbon (^{13}C), fluorine (^{19}F) and sodium (^{23}Na). However, the high sensitivity of the hydrogen (^{1}H) nucleus, its abundance within certain neurometabolites and the fact that the technique can be performed using standard clinical MR imaging machines makes hydrogen the principal nucleus brain (Glunde, Artemov *et al*. 2010; Harry, Semple *et al*. 2010).

The proton MR spectrum comprises a set of resonances (peaks) distributed along the x-axis, labeled in parts per million (ppm). The amplitude of the resonances is measured on the y-axis typically using an arbitrary scale (Kussman, Wypij *et al*. 2010). Three prominent peaks are consistently seen: N-acetylaspartate (NAA) at 2.02; Creatine (Cr) at 3.02; and Choline (Cho) at 3.2 when depicted in ppm (figure 1). Although the positions of the resonances along the x-axis are constant, the relative heights of the resonances can differ depending on various MR imaging parameters (Limperopoulos, Tworetzky *et al*. 2010).

Corresponding Author: Dr. Hany Kamal, Physics Department, Faculty of Science, Mansoura University, Mansoura 35516, Egypt.
E-mail: hkamal2000@gmail.com

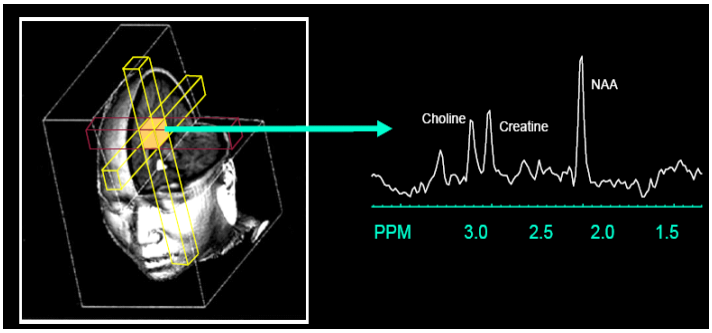

Fig. 1: MRS spectrum of a normal voxel.

Our aim was to focus on the potential of this technique to illustrate the role magnetic resonance spectroscopy in determining whatever there is a response for the treatment with radiation therapy or not. With this purpose, we developed studied two quantitative measurements techniques for six major metabolite resonances in multi-voxel MR spectra obtained from brain tumors at long echo time (144 ms), and compared their values among different voxels of patient. This method may help to obtain a calibration method used to check out the obtained data from MRS machine.

Experimental:

In order to generalize a single voxel MR spectroscopy, it is important to select a larger volume of interest and then apply phase encoding to obtain a localization one-, two-, or three-dimensional array of voxels. Point Resolved Spectroscopy (PRESS) or stimulated echo acquisition mode (STEAM) are the two most common methods used for volume selection, with PRESS being preferred when the echo time allows because of its intrinsically higher signal to noise ratio (Nelson 2003).

The reconstruction of MRS data and analysis of the resulting arrays of spectra combines Fourier transforms and apodization with automated methods of spectral processing to provide data that can be interpreted by visual inspection or quantified to generate maps of the spatial distribution of different metabolites. The first step is to apply an apodization function to the k-space-free induction decays and perform a Fourier transform to produce k-space spectra. The next step is to reconstruct the spatial dependence of the data. For spiral or irregular k-space sampling, the approach is to first re-grid the k-space data onto a rectangular array. For conventional phase encoding, this step is unnecessary (Nelson 2003). To center the data at the most appropriate spatial location, it is possible to phase-weight the k-space array with the appropriate voxel shift. This is followed by applying any required spatial apodization and then performing the spatial Fourier transformations. The resulting array of spectra will typically have spatially dependent frequency and phase errors that need to be corrected, as well as baseline variations because of residual water (Nelson 2003).

RESULTS AND DISCUSSION

In a proton spectrum at 1.5 T, the metabolites are spread out between the resonant frequencies 63MHz and 64 MHz. Metabolites may be positioned on a spectral line in their proper positions and expressed by parts per million (ppm) rather than use resonance frequencies (Glunde, Artemov *et al*. 2010). For example, N-acetylaspartate, or NAA, which is the second most abundant metabolite in the human central nervous system (CNS) positioned at 2.0 ppm on the scale (Panigrahy, Nelson Jr *et al*. 2010).

Protons present in different molecules resonate with slightly different frequencies because the magnetic field experienced by the proton inside voxel is affected by the electrons cloud inside it. Thus a Fourier transform is used to separate the signal into its individual frequencies (Limperopoulos, Tworetzky *et al*. 2010).

It is well known that imaging using MRS results from the signals obtained from all protons in the tissue (Bathen, Sitter *et al*. 2010). The signal obtained for MRS comes from fats and water are huge, thus the scaling to metabolites makes them invisible (Kussman, Wypij *et al*. 2010). In MRS, the signals that come from fats and mater are supposed to be eliminated. This can be done by placing the voxel of MRS within the brain away from bone marrow and scalp fats.

Normal MRS Spectrum obtained from gray matter and white matter. The predominant metabolites are NAA, creatine and choline are shown in figure 1. The primary difference between the two spectra is that gray matter has more creatine. The common way to analyze clinical spectra is to look at metabolite ratios, namely NAA/Cr, NAA/Cho, and Cho/Cr. By including a known reference (normal voxel) when acquiring the MR spectral data the absolute concentrations of metabolites can be directly calculated.

The water effect in brain was suppressed by using two techniques which are chemical-Shift selective (CHESS) or Inversion recovery (IR) techniques. Both of these techniques are used with a Stimulated Echo

Acquisition Mode (STEAM) or Point Resolved Spectroscopy (PRESS) pulse sequence acquisition (Bathen, Sitter *et al*. 2010). STEAM pulse sequence collect the signal like a gradient echo by 90º refocusing pulse and shorter echo times on the expense of less signal-to-noise is achieved. PRESS pulse sequence collect the signal like a gradient echo by 180º refocusing pulse (Pinto, Chung *et al*. 2011).Our data may be expressed by a chemical shift imaging which refers to multi-voxel MRS and the Spectroscopic imaging which display the data as an image with the signal intensity representing the concentration of a particular metabolite.

The echo time has an effect on the information obtained with MRS as in MRI (Gambarota, Mekle *et al*. 2009). As a general rule, the single voxel, short TE technique is used to make the initial diagnosis, because the signal-to-noise is high and all metabolites are represented. Multi-voxel, long TE techniques are used to further characterize different regions of a mass and to assess brain parenchyma around or adjacent to the mass (Harry, Semple *et al*. 2010). Multi-voxel, long TE techniques are also used to assess response to therapy and to search for tumor recurrence. With a short TE of 30 msec, metabolites with both short and long T2 relaxation times are observed. With a long TE of 270 msec, only metabolites with a long T2 are seen, producing a spectrum with primarily NAA, creatine, and choline. One other helpful TE is 144 msec because it inverts lactate at 1.3 ppm (Ricard, Idbaih *et al*. 2012).

Brain metabolites that are seen on the MRS appear at a specific ppm, and each one reflects specific cellular and biochemical processes. Choline is a measure of increased cellular turnover and is elevated in tumors and inflammatory processes. Creatine provides a measure of energy stores (Nachod 2012). NAA is a neuronal marker and decreases with any disease that adversely affects neuronal integrity. Despite of MRS metabolites provide powerful information, but unfortunately, many notable metabolites are not represented in brain MR spectra. Not all neurotransmitters are visible in MRS such as acetylcholine, dopamine, and serotonin. DNA, RNA, most proteins, enzymes, and phospholipids are missing. Either their concentrations are too low, or the molecules are invisible to MRS (Vagnozzi, Signoretti *et al*. 2010).

Multi-voxel spectroscopy is a best method to detect infiltration of malignant cells beyond the enhancing margins of tumors. Particularly in the case of cerebral glioma, elevated choline levels are frequently detected in edematous regions of the brain outside the enhancing mass. MRS can direct the surgeon to the most metabolically active part of the tumor for biopsy to obtain accurate grading of the malignancy (Nachod 2012).

A common clinical problem is distinguishing tumor recurrence from radiation effects several months following surgery and radiation therapy. Elevated choline is a marker for recurrent tumor. Radiation change generally exhibits low NAA, creatine, and choline on spectroscopy. MRS cannot always distinguish primary and secondary tumors of the brain from one another (Taylor, Quirke *et al*. 2011). Most non-glial tumors have little or no NAA. They also have no NAA, very low creatine, and elevated glutamates (Gujar, Maheshwari *et al*. 2005). The key feature of gliomas is elevated choline beyond the margin of enhancement due to infiltration of tumor into the adjacent brain tissue. If radiation necrosis is present, the spectrum may reveal elevated lipids and lactate.

Creatine (Cr) is also involved in the energy metabolism. The resonance marked with Cho consists of signals from choline (Cho), phosphorcholine (PC) and glycerolphosphocholine (GPC), which are markers for cell density and cell integrity. It is mainly found in glial cells and therefore considered to be a marker for glial proliferation. The resonance marked with NAA consists of signals from n-acetylaspartate and n-acetylaspartate glutamate, which are markers for viable neurons. The main function of glutamate (Glu) is that of a neurotransmitter and Glu is also part of the oxidative energy metabolism.

Besides the clear and high resonances of these metabolites, there are also a number of macromolecules and lipusedcerebelids present in the brain. Because of the short T_2 relaxation time of macromolecules and lipids, their signals are broad (Server, Josefsen *et al*. 2010).

Analyzes of patients who had abused radiotherapy sessions:

MRS can be used to determine the degree of malignancy. As a general rule, as malignancy increases, NAA and Creatine decrease, and choline, lactate, and lipids increase. NAA decreases as tumor growth displaces or destroys neurons. Very malignant tumors have high metabolic activity and deplete the energy stores, resulting in reduced creatine (Vagnozzi, Signoretti *et al*. 2010).Very hypercellular tumors with rapid growth elevate the choline levels. Lipids are found in necrotic portions of tumors, and lactate appears when tumors outgrow their blood supply and start utilizing anaerobic glycolysis. To get an accurate assessment of the tumor chemistry, the spectroscopic voxel should be placed over an enhancing region of the tumor, avoiding areas of necrosis, hemorrhage, calcification, or cysts (Haffner, Lemaitre *et al*. 2011).

Figure 2 shows the MRI for a brain tumor and table 1 shows the difference between the calculated and the measured brain metabolites directly from MRS. The tumor was determined from NMR image as seen in figure 2 and the voxels 5, 8, 9, 11 and 12 are located within the tumor area but the voxel number 16 is located in normal tissue and by drawing the spectrum between the intensity and concentration of the metabolites as in figure 3.

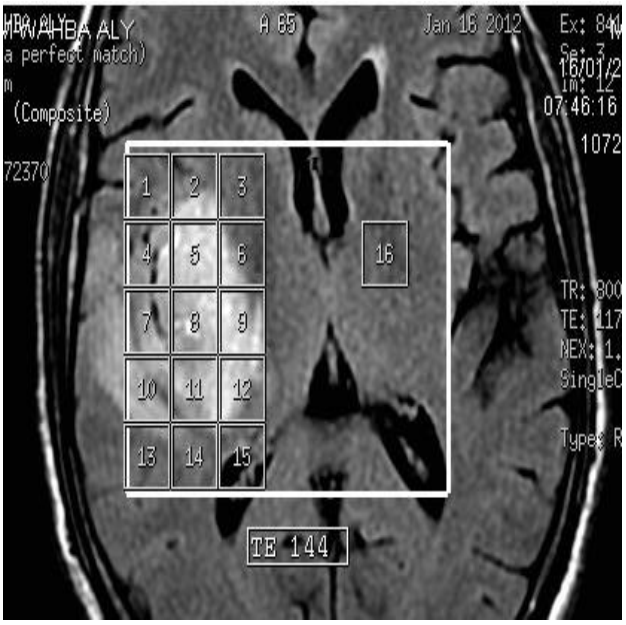

Fig. 2: MRI for a tumor in a brain has 16 voxels.

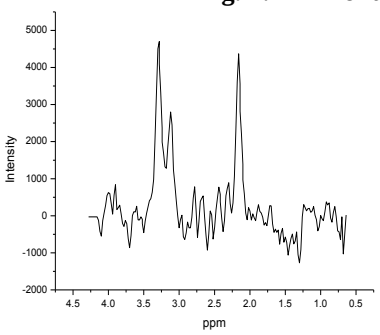

Voxel (5)

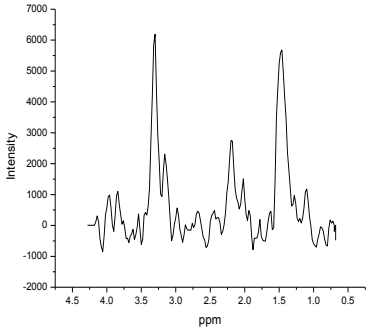

Voxel (8)

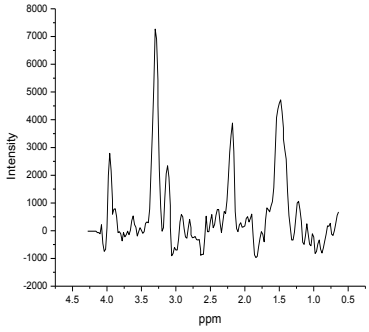

Voxel (9)

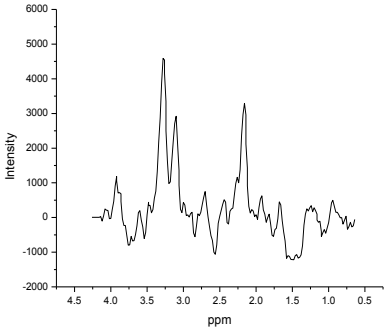

Voxel (11)

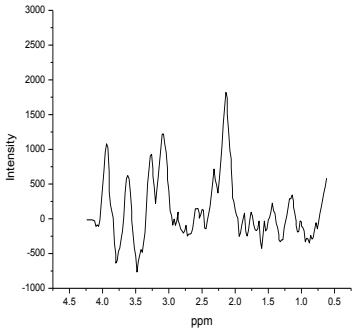

Voxel (12)

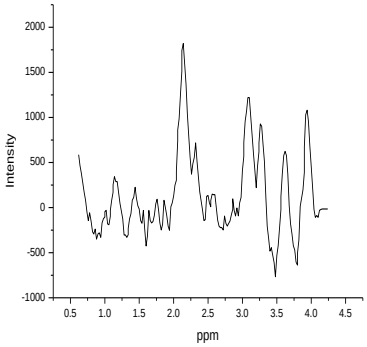

Voxel (16)

Fig. 3: MRS for a patient suffering from a tumor inside the brain before radiotherapy.

Table 1: Calculated and measured values from MRS for a patient suffering from a tumor inside the brain within a chosen voxels 5, 8, 9, 11 and 12 are located within the tumor area but the voxel number 16 is located in normal tissue.

metabolite	Abnormal Voxel (5)		Abnormal voxel (8)		Abnormal voxel (9)		Abnormal voxel (11)		Abnormal voxel (12)		Normal voxel (16)	
	Calcu-lated	MRS	Calcu-lated	MRS	Calcu-lated	MRS	Calcu-lated	MRS	Calcu-lated	MRS	Calcu-lated	MRS
Cho	11739	11737	29773	29766	38955	38962	43812	43802	31739	31702	6178	6171
Cr	12952	12947	18385	18392	13785	13794	13186	13189	19631	19602	10409	10406
NAA	22973	22968	25865	25872	20333	20328	23877	23892	21502	21516	15316	15312
Cr+Cho	24691	24684	48158	48158	52740	52756	56998	56991	51370	51304	16587	16577
Cho/Cr	0.9063	0.9065	1.6194	1.6184	2.8259	2.8246	3.3226	3.3211	1.6168	1.6173	0.5935	0.5930
Cho/NAA	0.5110	0.5110	1.1511	1.1505	1.9159	1.9167	1.8349	1.8333	1.4761	1.4734	0.4034	0.4030
NAA/Cho	1.9570	1.9569	0.8687	0.8692	0.5220	0.5217	0.5450	0.5455	0.6775	0.6787	2.4791	2.4813
NAA/Cr	1.7737	1.7740	1.4069	1.4067	1.4750	1.4737	1.8108	1.8115	1.0953	1.0976	1.4714	1.4715
Cr/NAA	0.5638	0.5637	0.7108	0.7109	0.6780	0.6786	0.5522	0.5520	0.9130	0.9110	0.6796	0.6796

Figure 4 shows that the ratios NAA/Cr, NAA/Cho, and Cho/Cr are 1.774, 1.9569 and 0.9065 respectively in voxel 5 as an example for the data measured from MRS. Figure 5 shows that the calculated values from the spectrum are very close to that measured where the values for NAA/Cr, NAA/Cho, and Cho/Cr are 1.7737, 1.9570 and 0.9063 respectively. For the normal voxel 16, the values that measured from MRS are 1.4715, 2.4813 and 0.5930 and the calculated values are 1.4714, 2.4791and 0.5935 respectively.

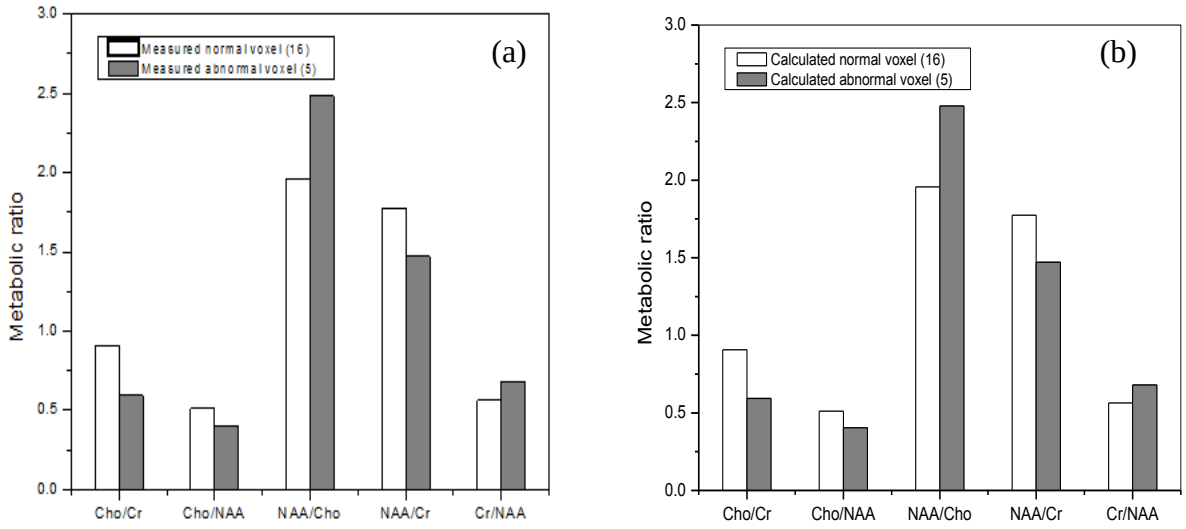

Fig. 4: Metabolic ratios Cho/Cr, Cho/NAA, NAA/Cho, NAA/Cr and Cr/NAA for abnormal voxel 5 and normal voxel 16 from MRS. (a) Measured, (b) Calculated.

Table 2 shows the percentage error $|\varepsilon\%|$ between measured from MRI and calculated values for the different metabolites for the abnormal voxels 5, 8, 9, 11 and 12 and the normal voxel 16.

Table 2: Percentage error $|\varepsilon\%|$ between measured from MRI and calculated values for the different metabolites.

Voxel Metabolite	Abnormal Voxel (5)	Abnormal Voxel (8)	Abnormal Voxel (9)	Abnormal Voxel (11)	Abnormal Voxel (12)	Normal Voxel (16)
Cho	0.0170	0.0235	0.0180	0.0228	0.1167	0.1134
Cr	0.0386	0.0381	0.0652	0.0227	0.1479	0.0288
NAA	0.0218	0.0271	0.0246	0.0628	0.0651	0.0261
Cr+Cho	0.0284	0.0000	0.0303	0.0123	0.1286	0.0603
Cho/Cr	0.0221	0.0618	0.0460	0.0452	0.0309	0.0843
Cho/NAA	0.0000	0.0522	0.0417	0.0873	0.1832	0.0993
NAA/Cho	0.0051	0.0575	0.0575	0.0917	0.1768	0.0887
NAA/Cr	0.0169	0.0142	0.0882	0.0386	0.2095	0.0068
Cr/NAA	0.0177	0.0141	0.0884	0.0362	0.2195	0.0000

The percentage errors for the different metabolites for the abnormal voxels 5, 8, 9, and 11 are less than 0.088%. For voxel 12 the percentage error is less than 0.22 %. The percentage error of the normal voxel (16) is less than 12 % for Cho and is less than 0.099% for other metabolites.

Figure 5 (a) shows that there is a good agreement between data measured form MRS with that calculated from the spectra for Cho, Cr and NAA of the same voxel which are 11737, 12947 and 22968 respectively in voxel 5. These values are very close to that calculated from spectrum which is for Cho, Cr and NAA which are

11739, 12952 and 22973 respectively. Figure 5 (b) for the normal voxel 16, the values that obtained from are MRS 6171, 10406 and 15312 and the calculated values are 6178, 10409 and 15316 respectively.

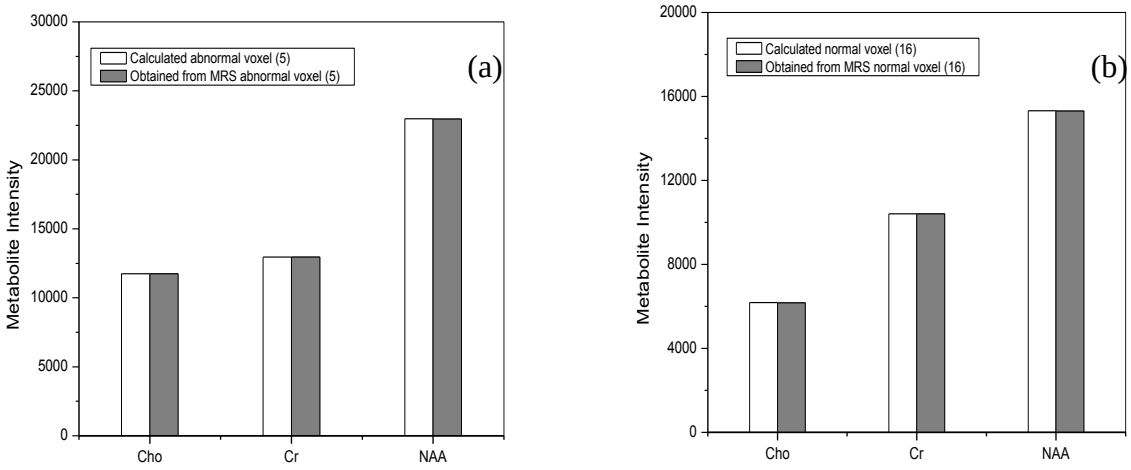

Fig. 5: Calculated and measured metabolic intensities of Cho, Cr and NAA. Abnormal Voxel (5) , (b) Normal Voxel (16).

The patient took radiotherapy sessions for two months and then followed by MRS and the data were analyzed by the same method used before. The obtained data from MRS and that calculated are given in table 3. It was found that peaks of both the lipids (Lip) and lactate (Lac) were higher after radiation therapy than before. Choline (Cho) is considered to be a marker of accelerated cell proliferation and high levels of choline have often been found in tumors (Righi, Andronesi *et al*. 2010). So Cho concentration is thought to be a useful marker for the evaluation of early post-radiation response. MRS *in vivo* in patients after brain tumor radiotherapy revealed a statistically significant decrease in the NAA/Cr ratio and increases in the Cho/ Cr, and Cho/NAA. High levels of lactate (Lac) have been found in tumors with a high malignancy grade (Haffner, Lemaitre *et al*. 2011). Also levels of the ratio of Cho to NAA can vary strongly within (tumor) tissue (Glunde, Artemov *et al*. 2010). In most cases a decrease of the signal intensity level of n-acetylaspartate (NAA) is detected for all tumor types. The area under the resonance peak in the spectrum is a measure for the tissue concentration of that specific molecule present in the assessed volume.

Table 3: Calculated and measured from MRS values for a patient who had taken radiation therapy sessions and suffering from a tumor inside the brain within a chosen voxels 57, 17, 24, 33 and 73 are located within the tumor area but the voxel number 81 is located in normal tissue.

metabolite	Abnormal Voxel (57)		Abnormal voxel (17)		Abnormal voxel (24)		Abnormal voxel (33)		Abnormal voxel (73)		Normal voxel (81)	
	Calc.	MRS	Calc.	MRS	Calc.	MRS	Calc.	MRS	Calc.	MRS	Calc.	MRS
Cho	12987	11981	31658	31640	39852	39832	45820	45801	32698	32680	18924	18908
Cr	12688	12662	18265	18259	13765	13732	13356	13341	19459	19440	0.7282	0.7284
NAA	18966	18981	23658	23642	18597	18576	22012	22042	20099	20110	0.5328	0.5333
Cr+Cho	25675	24643	49923	49899	53617	53564	59176	59142	52157	52120	1.8767	1.8748
Cho/Cr	1.0235	0.9462	1.7332	1.7328	2.8951	2.9006	3.4306	3.4331	1.6803	1.6810	1.3666	1.3658
Cho/NAA	0.6847	0.6312	1.3381	1.3382	2.1429	2.1442	2.0815	2.0778	1.6268	1.6250	0.7317	0.7321
NAA/Cho	1.4603	1.5842	0.7472	0.7472	0.4666	0.4663	0.4804	0.4812	0.6146	0.6153	18924	18908
NAA/Cr	1.4947	1.4990	1.2952	1.2948	1.3510	1.3527	1.6480	1.6522	1.0328	1.0344	0.7282	0.7284
Cr/NAA	0.6689	0.6670	0.7720	0.7723	0.7401	0.7392	0.60676	0.6052	0.9681	0.9666	0.5328	0.5333

Table 4: Percentage error $|\varepsilon\%|$ between measured from MRI and calculated values for the different metabolites.

Metabolite	Abnormal voxel (57)	Abnormal voxel (17)	Abnormal voxel (24)	Abnormal voxel (33)	Abnormal voxel (73)	Normal voxel (81)
	$\|\varepsilon\%\|$	$\|\varepsilon\%\|$	$\|\varepsilon\%\|$	$\|\varepsilon\%\|$	$\|\varepsilon\%\|$	$\|\varepsilon\%\|$
Cho	0.0462	0.0569	0.0502	0.0415	0.0551	0.0846
Cr	0.2053	0.0329	0.2403	0.1124	0.0977	0.0275
NAA	0.0790	0.0677	0.1130	0.1361	0.0547	0.0938
Cr+Cho	0.1248	0.0481	0.0989	0.0575	0.0710	0.1013
Cho/Cr	0.1561	0.0231	0.1896	0.0728	0.0416	0.0586
Cho/NAA	0.1316	0.0075	0.0606	0.1781	0.1108	0.0546
NAA/Cho	0.1299	0.0000	0.0643	0.1663	0.1138	0.0846
NAA/Cr	0.2869	0.0309	0.1257	0.2542	0.1547	0.0275
Cr/NAA	0.2849	0.0388	0.1218	0.2578	0.1552	0.0938

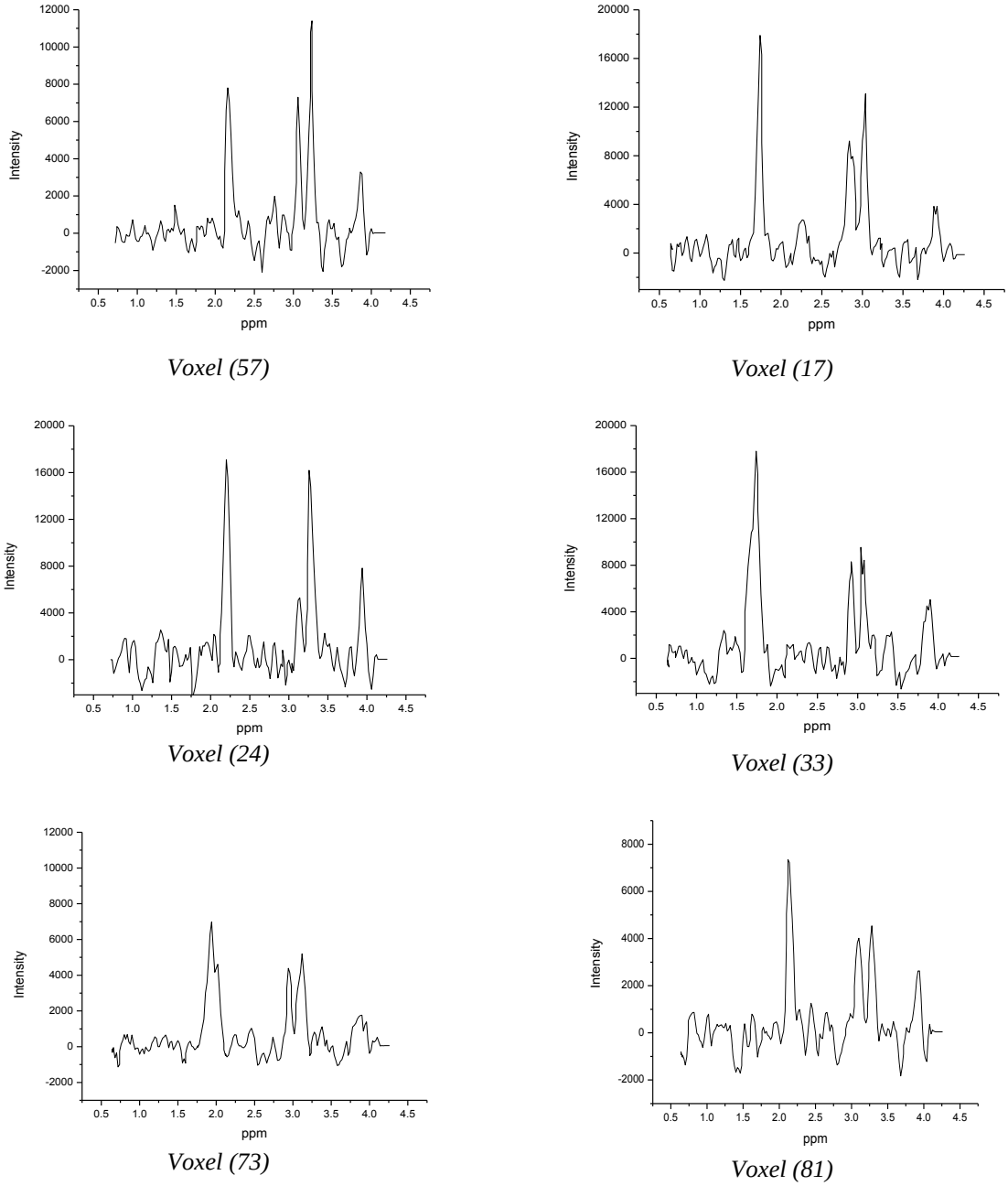

Fig. 6: MRS for a patient suffering from a tumor inside the brain after radiotherapy.

The percentage errors for the different metabolites of the abnormal voxels 57, 17, 24, 33 and 73 are less than 0.286%. For normal voxel 81 the percentage error is less than 0.093 % for NAA and is less than 0.084% for other metabolites.

In figure 7, a plot of metabolic intensities of Cho, Cr, and NAA before and after radiation sessions. It was noted that the level of Cho increase after radiation sessions and that of NAA decreases and there is a good agreement between data form MRS with that calculated from spectra for Cho, Cr and NAA and that obtained from spectra of Cho, Cr and NAA from MRS. ^{1}H MRS of single voxels localized inside the core of the tumor has been used to establish in vivo MR spectral profiles of specific tumor types (Elias, Carlos *et al*. 2011). The average metabolite profiles from short and long echo time MR spectra were derived from these measurements and one can clearly see differences between the profiles of tumors and of normal brain.

Loss of neuronal integrity is usually mentioned as being the cause of the decreased NAA concentration in the brain. NAA is a marker for viable neurons, and it is not present in tumor tissue (Server, Josefsen *et al*. 2010). An increased level of lipids is generally found in tumors with necrotic tissue. Lipids are present due to breakdown of the membranes of dead cells (Morita, Harada *et al*. 2010). It well known that metabolic changes have been related to tumor grade. Choline has been associated with cell proliferation. This was a reason to

investigate the relation between the levels of these metabolites and malignancy grade of the tumor since tumors cells often have a high level of proliferation. It was found that the levels of choline and myo-inositol are higher in tumors with a higher malignancy grade (Ricard, Idbaih *et al*. 2012). The level of glycine has also been related to the grade of the tumor, however, the exact role of glycine in brain tumors has sparsely been evaluated (Shenton, Hamoda *et al*. 2012).

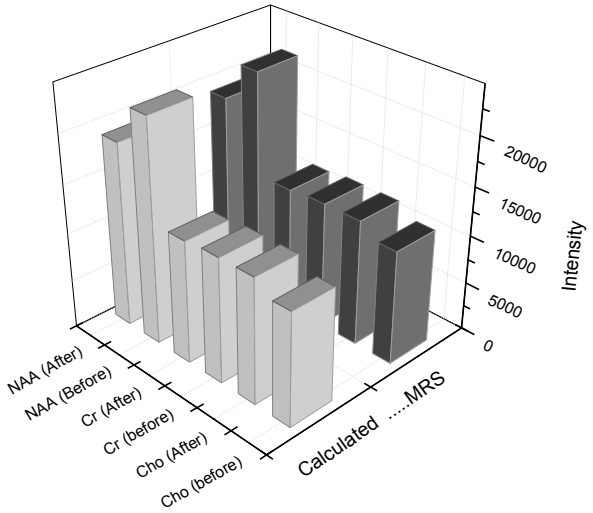

Fig. 7: A plot of metabolic intensities of Cho, Cr and NAA before and after radiation sessions. The white columns are for calculated values for normal voxel 5 and gray ones are for obtained directly from MRS for the same normal voxel 5.

Another important feature of malignant tumor types is the presence of lipids. Lipids accumulate in the brain due to necrosis (cell death) and a relation has been found between lipids and features of tumor malignancy such as necrosis (Shenton, Hamoda *et al*. 2012).

In several studies metabolite levels have been related to the presence of tumor cells indifferent brain tissue. This has been done by relating deviations from specific metabolite ratios (for example the ratio of Cho to NAA) to the presence of tumor cells in a tissue biopsy sample obtained from the same location as recorded by in vivo MRS. Also the level of choline in MR spectra has been related to tumor cell density of the biopsy specimens from similar locations (Zhou, Tryggestad *et al*. 2011). These results were very promising with respect to using the level of choline to predict tumor presence, despite potential problems such as inaccurate registration of the location from which the tissue specimens and MR spectra were obtained, and the difference in volume of biopsies and MRS voxels. A part from choline, only a few other metabolic changes have been observed in the peripheral zone of glial tumors. Unfortunately, these changes are not very obvious and therefore the peripheral tumor zone remains an ongoing subject of research.

Conclusions:

From the study that has been performed, it is clear that MRS is an important to evaluate the response to therapy. Also it is important for choosing the most appropriate therapy for individual patients and for understanding the mechanisms of success and failure of new treatments. The good agreement between the data obtained from MRS and that calculated from their spectra help to trust the data from MRS machine. Therefore, this method can be used to calibrate the MRS device before use on a standard sample and thus check the sensitivity of MRS machine. This could be a critical for screening therapies based upon the biological properties of the tumor, where it is important to know whether the lack of response was because of the agent being unable to access the tumor or to the lesion being insensitive to that particular approach.

REFERENCES

Bathen, T.F., B. Sitter, *et al*., 2010. "Magnetic resonance metabolomics of intact tissue: a biotechnological tool in cancer diagnostics and treatment evaluation." Cancer research, 70(17): 6692-6696.

Chiang, I., T. Hsieh, *et al*., 2014. "Distinction between pyogenic brain abscess and necrotic brain tumour using 3-tesla MR spectroscopy, diffusion and perfusion imaging."

Elias, A.E., R.C. Carlos, *et al*., 2011. "MR spectroscopy using normalized and non-normalized metabolite ratios for differentiating recurrent brain tumor from radiation injury." Academic radiology, 18(9): 1101-1108.

Gambarota, G., R. Mekle, *et al*., 2009. "In vivo measurement of glycine with short echo-time 1H MRS in human brain at 7 T." Magnetic Resonance Materials in Physics, Biology and Medicine, 22(1): 1-4.

Glunde, K., D. Artemov, *et al*., 2010. "Magnetic resonance spectroscopy in metabolic and molecular imaging and diagnosis of cancer." Chemical reviews, 110(5): 3043-3059.

Gujar, S.K., S. Maheshwari, *et al*., 2005. "Magnetic resonance spectroscopy." Journal of neuro-ophthalmology, 25(3): 217-226.

Haffner, J., L. Lemaitre, *et al*., 2011. "Role of magnetic resonance imaging before initial biopsy: comparison of magnetic resonance imaging-targeted and systematic biopsy for significant prostate cancer detection." BJU international, 108(8b): E171-E178.

Harry, V.N., S.I. Semple, *et al*., 2010. "Use of new imaging techniques to predict tumour response to therapy." The lancet oncology 11(1): 92-102.

Kussman, B.D., D. Wypij, *et al*., 2010. "Relationship of intraoperative cerebral oxygen saturation to neurodevelopmental outcome and brain magnetic resonance imaging at 1 year of age in infants undergoing biventricular repair." Circulation, 122(3): 245-254.

Limperopoulos, C., W. Tworetzky, *et al*., 2010. "Brain volume and metabolism in fetuses with congenital heart disease evaluation with quantitative magnetic resonance imaging and spectroscopy." Circulation, 121(1): 26-33.

Morita, N., M. Harada, *et al*., 2010. "Clinical application of MR spectroscopy and imaging of brain tumor." Magnetic Resonance in Medical Sciences, 9(4): 167-175.

Nachod, F.C., 2012. Determination of organic structures by physical methods, Elsevier.

Nelson, S.J., 2003. "Multivoxel Magnetic Resonance Spectroscopy of Brain Tumors1." Molecular Cancer Therapeutics, 2(5): 497-507.

Panigrahy, A., M.D. Nelson Jr, *et al*., 2010. "Magnetic resonance spectroscopy in pediatric neuroradiology: clinical and research applications." Pediatric radiology, 40(1): 3-30.

Pinto, P.A., P.H. Chung, *et al*., 2011. "Magnetic resonance imaging/ultrasound fusion guided prostate biopsy improves cancer detection following transrectal ultrasound biopsy and correlates with multiparametric magnetic resonance imaging." The Journal of urology, 186(4): 1281-1285.

Ricard, D., A. Idbaih, *et al*., 2012. "Primary brain tumours in adults." The Lancet, 379(9830): 1984-1996.

Righi, V., O.C. Andronesi, *et al*., 2010. "High-resolution magic angle spinning magnetic resonance spectroscopy detects glycine as a biomarker in brain tumors." International journal of oncology, 36(2): 301-306.

Server, A., R. Josefsen, *et al*., 2010. "Proton magnetic resonance spectroscopy in the distinction of high-grade cerebral gliomas from single metastatic brain tumors." Acta Radiologica, 51(3): 316-325.

Shenton, M., H. Hamoda, *et al*., 2012. "A review of magnetic resonance imaging and diffusion tensor imaging findings in mild traumatic brain injury." Brain imaging and behavior, 6(2): 137-192.

Taylor, F.G., P. Quirke, *et al*., 2011. "Preoperative high-resolution magnetic resonance imaging can identify good prognosis stage I, II, and III rectal cancer best managed by surgery alone: a prospective, multicenter, European study." Annals of surgery, 253(4): 711-719.

Vagnozzi, R., S. Signoretti, *et al*., 2010. "Assessment of metabolic brain damage and recovery following mild traumatic brain injury: a multicentre, proton magnetic resonance spectroscopic study in concussed patients." Brain: awq200.

Zhou, J., E. Tryggestad, *et al*., 2011. "Differentiation between glioma and radiation necrosis using molecular magnetic resonance imaging of endogenous proteins and peptides." Nature medicine, 17(1): 130-134.